Portugaliae Electrochimica Acta 2020, 38(2), 125-138

DOI: 10.4152/pea.202002125

PORTUGALIAE ELECTROCHIMICA ACTA
ISSN 1647-1571

Synthesis and comparative study between two pyrazoles in inhibition against the corrosion of steel in 1 M hydrochloric acid

R. Chadli,[a,*] M. Elazouzi,[b] I. Khelladi,[c] A.M. Elhorri,[d] J. Kajima Mulangi,[a] B. Hammouti[b] and A. Aouiniti[b]

[a] *Department of Chemistry, Faculty of Exact Sciences, Djillali Liabes University of Sidi Bel Abbes, 22000, Algeria*
[b]*Laboratoire de chimie organique, substances naturelles & analyse (COSNA), Department of Chemistry, Faculty of Exact Sciences, University Abo uBeker Bel Kaid, Tlemcen, Algeria*
[b]*Laboratoire de chimie appliquée et envérennement (LCAE-URAC18), Faculty of Sciences, Oujda, Maroc*
[c]*Laboratoire de microscopie, microanalyse de la matière et spectroscopie moléculaire, Department of Chemistry, Faculty of Exact Sciences, University Djilali Liabes Sidi BelAbbes, Algeria*
[d]*Department of Chemistry, Faculty of Exact Sciences and Informatics, Hassiba Ben Bouali University of Chlef, P.O. Box 78C, Ouled Fares Chlef 02180, Algeria*

Received February 15, 2019; accepted June 06, 2019

Abstract

In this work we made a synthesis of two molecules of the same family, the pyrazole 4-(4,5-dihydro-1H-pyrazol-5-yl)-N,N-dimethylaniline D and N,N-dimethyl-4-(3-methyl-4,5-dihydro-1H-pyrazol-5-yl)aniline D10. These two molecules have a good inhibiting activity against the corrosion of mild steel in 1 M HCl. This activity has been confirmed by gravimetric and electrochemical studies; we use a potentiodynamic polarization and the impedance spectroscopic technique. From this investigation, we observe that the integration of a methyl group in the pyrazole D allows decreasing slightly the corrosion of steel. For more information about the action mode of our inhibitors, we launched theoretical calculation by DFT method. We used these calculations to discuss the stability, the reactivity, and the adsorption of our pyrazolic inhibitors with iron in acid medium.

Keywords: Mild steel, pyrazole; hydrazine, hydrazones, corrosion inhibition, DFT.

Introduction

Pyrazoles are an important class of heterocyclic compounds. They are used in several domains of current research; for example, we found pyrazole derivatives with biological activities such as antitumor [1,2], antibacterial [3], anticancer [4], antidiabetic agent [5], anti-inflammatory [6], antidepressant [7], antimalaria [8],anticonvulsant [9], antituberculosis [10] and antiviral activities [11].

[*] Corresponding author. E-mail address: redouane.chadli@univ-sba.dz & mailchadli@yahoo.fr

On the other hand, there is a very important number of substituted pyrazoles which have a broad spectrum at the industrial activities [12], especially in the corrosion inhibitors for steel in acidic media [13-17]. Bibliography results directed us towards the synthesis of new pyrazole derivatives. This synthesis has been followed by a gravimetric test; this test makes it possible to observe the influence of pyrazoles concentration on the corrosion rate of mild steel in an acid medium. The protection of iron against corrosion is very important, because the use of metals touches almost all the domains of our life such as mechanics, industry, electro-household and construction of buildings. The iron is prone by several parameters and conditions of corrosion that limit its use [18-24]. The use of organic inhibitors against corrosion of steel is advantageous from the point of view of cost, quantity and efficiency. These organic inhibitors are usually adsorbed onto the metal surface via formation of a coordinate-covalent bond (chemical adsorption) or the electrostatic interaction between the metal and inhibitor (physical adsorption) [25]. To confirm and evaluate the inhibitory activity of the corrosion of an organic molecule, we use gravimetric (loss of weight) and electrochemical studies (polarization and impedance spectroscopy). The inhibition mechanism can be justified by thermodynamic studies (Temkin, Frumkin and Langmuir) and by molecular parameters calculated by DFT method [26]. These two studies give a simulation of the adsorption of the inhibitor molecules on the metal surface.

In this work we made the synthesis of the pyrazoles[4-(4,5-dihydro-1H-pyrazol-5-yl)-N,N-dimethylaniline] **D** and [N,N-dimethyl-4-(3-methyl-4,5-dihydro-1H-pyrazol-5-yl)aniline] **D10**, by a reaction between hydrazine and the carbonyl α,β-unsaturated such as 3-(4-(dimethylamino)phenyl)acrylaldehyde and 4-(4-(dimethylamino)phenyl)but-3-en-2-one in the alcohol as solvent. These reactions give the pyrazole with an excellent yield because there is a good reactivity of hydrazine [27-32] (Fig. 1).

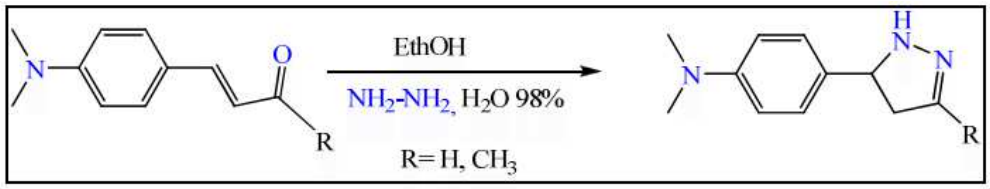

Figure 1. Effected synthesis of pyrazoles.

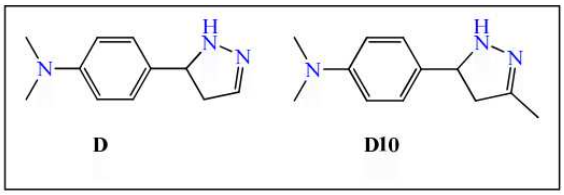

Figure 2. Chemical structure of **D** and **D10**.

The second objective of this work is to investigate the corrosion of steel in 1 M HCl in the absence and presence of different concentrations of **D** and **D10,** (**D** and **D10** have the same chemical structure inserting a methyl group in the position 3 of the pyrazole (Fig. 2)). The inhibition efficiency of these compounds

was determined by using potentiodynamic polarization, electrochemical impedance spectroscopy and weight loss methods. The thermodynamic parameters and activation of inhibitor were studied.

Materials and methods

Materials

The I.R. spectra were performed in a Mattson Genesis *II FTIR* instrument. The NMR spectra were recorded in $CDCl_3$ in a Bruker *300 MHz* instrument. Melting points were determined in an Electrothermal *T1A F3.15A* instrument.

Synthesis of pyrazoles D and D10

These products were prepared by mixing 3-(4-(dimethylamino)-phenyl)-acrylaldehyde or 4-(4-(dimethylamino)phenyl)but-3-en-2-one (0.1 mol) dissolved in ethanol (100 mL). The solution of hydrazine sulphate (0.1 mol), soud (0.11 mol) and sodium iodide (0.01 mol) in water, was added drop-wise followed. The reaction mixtures were stirred for 24 hours without heating. In the end, the reaction mixture was cooled and poured in ice-cold water, and the precipitate formed was filtered off, washed and recrystallized in ethanol to get the corresponding pyrazole.

4-(4,5-dihydro-1H-pyrazol-5-yl)-N,N-dimethylaniline D

Yield (76%); m.p=142–144°C;IR(KBr, λmax): 3159, 3066, 2933, 1649, 1531, 1597cm^{-1}, ^{1}HNMR(CDCl3)δ: 2.95 (t,2H,CH_2),3.08 (s,6H,CH_3), 5.32 (s,1H,NH), 6.62 (t,1H,pyrazole CH),7.17–7.54 (m,4H,ArH), 8.44 (t,1H,CH)ppm; ^{13}CNMR($CDCl_3$): δ40.24, 111.73, 112.01, 123.64, 129.84, 151.76, 162.39ppm.

N,N-dimethyl-4-(3-methyl-4,5-dihydro-1H-pyrazol-5-yl)aniline D10

Yield (80%); m.p=217–219°C; IR(KBr, λ_{max}): 3205, 3080, 2933, 1665, 1610, 1440, 1395, 1320cm^{-1}. ^{1}H NMR($CDCl_3$)δ: 1.59 (s, 3H, CH_3), 0.8 (d, 2H, CH_2), 1.26 (s, 6H, CH_3), 1.8 (m, 1H, CH), 7.33-8.23 (m, 4H, ArH), 1.25 (s, 1H, NH) ppm; ^{13}CNMR($CDCl_3$)δ:20.1, 35.1, 61.0, 98.6, 120.5, 123.9, 129.1, 135.9, 146.5, 149.2,150.7, 161.2ppm.

Gravimetric, R_p polarization and EIS measurements

Steel samples *CX38* are used. The acidic solution was prepared by the dilution of 37% HCl analytical grade with bidistilled water. Prior to all measurements, the steel samples were polished with different emery paper up to 1200 grade and washed thoroughly with bidistilled water and dried with acetone. The concentration range of green inhibitor ranged within 10^{-3} and 10^{-6}M.

Gravimetric measurements

The weight loss is followed by a balance with an accuracy of 10^{-4} g. The volume of the solution is 250 mL. The steel used has a cylindrical shape (R = 2 cm and h = 0.5 cm). The immersion time for weight loss is 6 h at 25 °C.

Electrochemical measurements

The electrochemical experiments were recorded using an EG&G Instruments *potentiostat galvanostat model 263A,* at a scan rate of 0.5m V/s, coupled to a computer equipped with a *352SoftCorrIII* software. Before recording the polarization curves, the test solution was de-aerated and magnetically stirred for 30 min in the cell with pure nitrogen to attain stationary (E_{corr}). Gas bubbling was maintained throughout the experiments. The WE was then inserted and prepolarized at -800 mV (SCE) for 30 min in order to remove the oxide film from the electrode. The scan rate was 1 $mV.s^{-1}$. Polarization resistance measurements were performed by scanning through a potential range, which is very close to the corrosion potential. The potential range is ±10 mV around E_{corr}. Polarization resistance (R_P) values are obtained from the current potential plots. The temperature was thermostatically controlled at 25 °C.

Electrochemical impedance spectroscopy (EIS) measurements

EIS measurements were carried out with an electrochemical system (*Tacussel*) which included a digital potentiostat model *VoltalabPGZ100* computer, at E_{corr} after immersion in the solution without bubbling. A circular surface of 1 cm^2 steel exposed to the solution was used as the working electrode. After the determination of the current steady-state at a given potential, sinus wave voltage (10 mV) peak to peak, at frequencies between 100 kHz and 10 MHz, were superimposed on the rest potential. Computer programs automatically controlled the measurements performed at rest potentials after 10 min of exposure. The impedance diagrams are given in the Nyquist representation.

Table 1. Mathematic equations used in our calculus.

Energetic Parameter	*Symbol*		*Mathematic equation*
Ionization potential	*IE*	*eV*	$IE = -E_{HOMO}$
Electron affinity	*EA*	*eV*	$EA = -E_{LUMO}$
Gap energy	E_{gap}	*eV*	$Egap = IE + EA$
Electronegativity	χ	*eV*	$\chi = 0{,}5.(IE + EA)$
Global hardness	η	*eV*	$\eta = 0{,}5.(IE - EA)$
Softness	σ	eV^{-1}	$\sigma = \eta^{-1}$
Fraction of electrons transferred	ΔN		$\Delta N = 0{,}5\,.(\chi_{Fe} - \chi_{inh})(\eta_{Fe} + \eta_{inh})^{-1}$ with $\chi_{Fe} = 7eV$ and $\eta_{Fe} = 0$ [40]

Quantum chemical calculations

Theoretical calculations were carried out by Gaussian 03 package [33]. All geometries were optimized by DFT (Density Functional Theory) method. We used the most popular functional B3LYP [34-36] combined with 6-31G (d) basis-set. From the obtained geometries, we calculated by Single Point calculation the following parameters: the highest occupied molecular orbital $\mathbf{E_{HOMO}}$ and lowest unoccupied molecular orbital $\boldsymbol{E_{LUMO}}$ energies, the Gap $\mathbf{\Delta E_{H\text{-}L}}$/or $\mathbf{E_{gap}}$ between $\mathbf{E_{HOMO}}$ and $\mathbf{E_{LUMO}}$, the dipole moment $\boldsymbol{\mu}$, the electronegativity $\boldsymbol{\chi}$, the hardness $\boldsymbol{\eta}$, softness $\boldsymbol{\sigma}$ and fraction of electrons transferred $\mathbf{\Delta N}$. Table **1** presents the equations used for the calculation of different quantum chemical parameters of

the inhibitors **D** and **D10**. These parameters have been used to understand the properties and the activity of the new prepared compounds and to help in the explanation of the experimental data obtained for the corrosion process [37-39].

Results and discussion

Weight loss measurements

The corrosion rate (W_{corr}) of steel in 1 M HCl solution at various concentrations of the inhibitor was determined after 6 h of immersion period at 25 °C. The corrosion rate (W_{corr}) was calculated using the following equation:

$$W = \Delta m/S.t \quad (1)$$

where (Δm) is the average weight loss, (S) the total area, and t is immersion time. The values of corrosion rates and inhibition efficiencies are given in Table 2. In the case of the weight loss method, the inhibition efficiency ($E_W\%$) was determined by the following relation:

$$E_W\% = [(W_{corr} - W'_{corr})/W_{corr}].100 \quad (2)$$

Table 2. Weight loss data for mild steel 1 M HCl without and with different concentrations of **D** and **D10** at 25 °C.

	C (M)	Corrosion rate W'_{corr} (g/m².h)	Efficiency E_W(%)
HCl	-	9.04	**-**
D	10^{-6}	2.70	**70**
	5.10^{-6}	2.32	74
	10^{-5}	1.73	**80**
	5.10^{-5}	1.58	**82**
	10^{-4}	1.51	83
	5.10^{-4}	0.85	**90**
	10^{-3}	0.39	**96**
D10	10^{-6}	2.02	**77**
	5.10^{-6}	1.49	83
	10^{-5}	1.01	88
	5.10^{-5}	0.92	89
	10^{-4}	0.87	**90**
	5.10^{-4}	0.63	93
	10^{-3}	0.45	**95**

where W_{corr} is the corrosion rate of steel in 1 M HCl and W'_{corr} is the corrosion rate of steel with the inhibitors.

It had been observed that the inhibition efficiency increased with increasing concentration and reached a maximum value at an optimum concentration of 10^{-3} M.

We noted that our compounds used in this study showed very good inhibition of corrosion and the inhibition efficiency increases with the increase of the inhibitor concentration. Generally, organic inhibitors suppress the metal dissolution by forming a protective film adsorbed onto the metal surface and separating it from the corrosion medium [40].

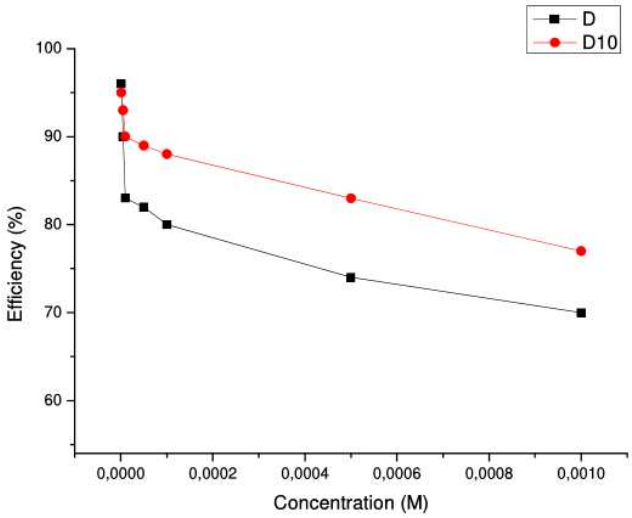

Figure 3. Variation of the inhibition efficiency with concentration of the inhibitors

The inhibition efficiency attains 96% and 95% for **D** and **D10**, respectively. Thus, we deduce that **D** is the best inhibitor of these two tested compounds (Fig. 3). The variation in inhibitive efficiency mainly depends on the type and the nature of the substituents present in the inhibitor molecule. This difference in efficiency could be explained by computational calculations using *DFT* method (see the last part of this work).

Polarization measurements

Fig. 4 presents the Tafel polarization curves for steel in 1 M HCl for different concentrations of **D** and **D10** molecules. Table 3 lists the values of E_{corr} (corrosion potential), I_{corr} (corrosion current density), and β_c (Tafel cathodic constant).The inhibition efficiency was calculated using the corrosion current densities measurements, I_{corr}, for steel electrode according to the following equation:

$$E_p\,\% = [(I_{corr} - I_{corr(inh)})/\, I_{corr}].\,100 \qquad (3)$$

where I_{corr} is the corrosion current density for steel in 1 M HCl, and $I_{corr(inh)}$ is the corrosion current density for steel electrode in 1 M HCl solution with the inhibitors **D** and **D10**. As can been seen from Fig. 4, it is clear that both anodic and cathodic reactions of the corrosion process were inhibited when the pyrazole derivatives were added to the acid solution.

The cathodic polarization curves of our inhibitors are almost parallel. The corrosion potential of mild steel shifted to the negative side only 53 mV for **D** and 28 mV (vs. SCE) for **D10**. This value indicates that the addition of our

inhibitors to the acid solution does not change the mechanism of the cathodic reaction (hydrogen evolution) [41].

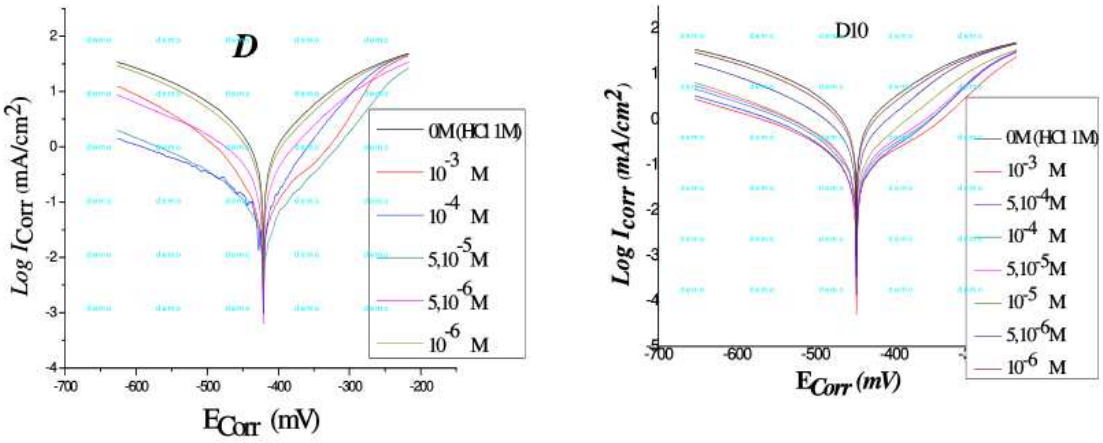

Figure 4. Typical polarization curves for mild steel in 1 M HCl for various concentrations of **D** and **D10** at 25 °C.

Table 3. Electrochemical parameters derived from polarization measurements for mild steel in 1 M HCl solution in the absence and presence of various concentrations of **D** and **D10**.

	C (M)	**E_{corr} (mV *vs.* CSE)**	**I_{corr} (µA/cm²)**	**$-\beta_c$ (mV/dec)**	**β_a (mV/dec)**	**R_p (Ω/cm²)**	**E_p (%)**
HCl	1	-450	2512	140	185	20.14	/
D	10^{-3}	-421	41	87.5	62.6	167.66	**98**
	10^{-4}	-464	81	115.4	91.9	289.68	97
	5.10^{-5}	-463	87	119.2	129.4	328.01	96
	5.10^{-6}	-474	285	101.7	76.8	59.15	88
	10^{-6}	-452	560	74.8	79.7	26.35	77
D10	10^{-3}	-480	41	125.5	72.6	387.98	**98**
	5.10^{-4}	-467	65	136.3	71.8	233.47	97
	10^{-4}	-473	167	153.6	86	169.82	93
	5.10^{-5}	-477	198	152.6	90.4	158.89	92
	10^{-5}	-457	454	184.6	103.3	114.20	81
	5.10^{-6}	-452	1401	188.8	124.1	49.06	44

We noticed that the addition of our inhibitors in the aggressive medium causes a remarkable decrease in the corrosion rate, shifting both anodic and cathodic Tafel curves to lower current densities. This phenomenon indicates that both anodic and cathodic reactions are suppressed and the suppression effect becomes more pronounced with the increase of the concentration of these inhibitors.

Electrochemical impedance spectroscopy

The corrosion of mild steel in 1 M HCl solution in the presence of ours inhibitors were investigated by *EIS* at room temperature after an exposure period of 30 min. Nyquist plots for mild steel obtained at the interface in the absence and presence of this inhibitor at different concentrations are illustrated in Fig. 5.The addition

of the inhibitors increases the capacitive loop diameter without affecting their characteristic features. This indicates the strengthening of the formed inhibitive film that is responsible for the inhibition action of these inhibitors [42]. The protective film is formed as a result of adsorption of inhibitor molecules on the carbon steel surface without changing the mechanism of the corrosion process. The inhibition efficiency was calculated using charge transfer resistance according to the following equation:

$$\mathbf{EI} = [(R_{t(inh)} - R_t)/R_{t(inh)}].100 \quad (4)$$

where R_t and $R_{t(inh)}$ are the charge transfer resistance values in the absence and presence of the inhibitor, respectively.

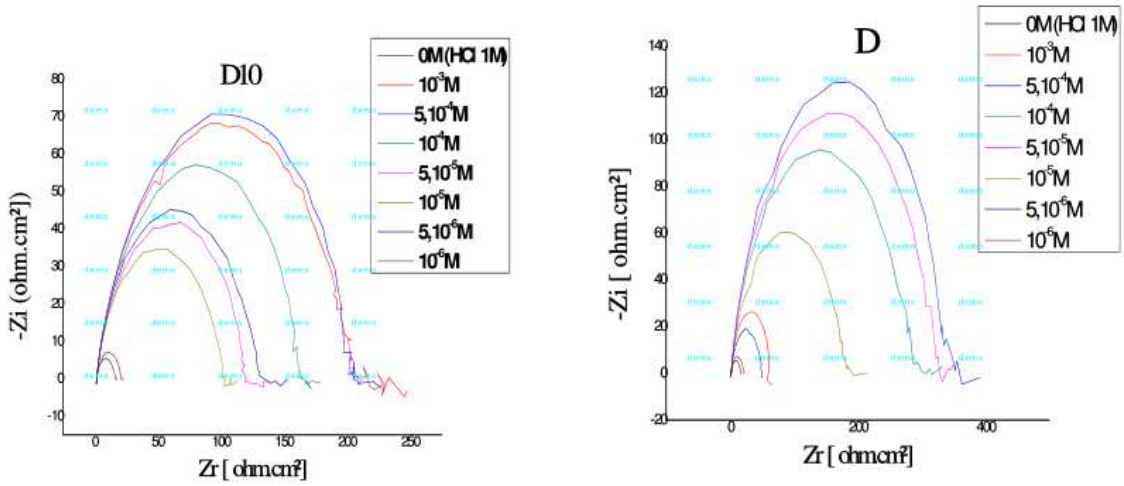

Figure 5. Nyquist plots for mild steel in 1 M HCl solution in presence of (**D**) and (**D10**).

Table 4. EIS parameters for corrosion of carbon steel in 1 M HCl in the absence and presence of different concentrations of the **D** and **D10** at 25 °C.

	C (M)	R_s	R_t *(Ω.cm²)*	C_{dl} *(μF.cm⁻²)*	E_I *(%)*
HCl	**Blank**	1.64	14.53	173	/
D	10^{-3}	-0.187	456.9	43.0	**97**
	5.10^{-4}	1.535	342	46.5	96
	10^{-4}	0.974	320.3	56.5	95
	5.10^{-5}	0.6192	323.3	65.3	95
	10^{-5}	1.062	179.5	75.5	92
	5.10^{-6}	1.609	48.09	82.8	70
	10^{-6}	1.542	20.02	158.9	27
D10	10^{-3}	1.479	260.5	61.07	**94**
	5.10^{-4}	1.085	206.3	61.1	93
	10^{-4}	1.198	164.5	61.7	91
	5.10^{-5}	1.388	119.4	66.6	88
	10^{-5}	1.391	100.9	78.9	85
	5.10^{-6}	1.547	38.42	103.5	62
	10^{-6}	1.630	20.04	158.7	27

Various impedance parameters such as charge transfer resistance (R_t), double layer capacitances (C_{dl}) and inhibition efficiency (E_I) were calculated and are listed in Table 4.
The addition of the inhibitors increases clearly the charge transfer resistance (R_t) values. This indicates the strong adsorption of our inhibitors with metal surface. The capacitance C_{dl} values were decreased due to a decrease in local dielectric constant and/or an increase in the thickness of the electrical double layer, suggesting that the inhibitor molecules acted by adsorption at the metal/solution interface. The addition of our inhibitors provided lower C_{dl} values, probably because of the replacement of water molecules by inhibitor molecules at the electrode surface. In addition, the inhibitor molecules may reduce the capacitance by increasing the double layer thickness [43].

Adsorption isotherm

Organic corrosion inhibitors decrease metal dissolution via adsorption on the metal/solution interface to form a protective film. The adsorption route is generally considering as a substitution process between the organic inhibitor in the aqueous solution and water molecules adsorbed at the metal surface [44]. The adsorption isotherm can give information on the metal–inhibitor interaction. Several adsorption isotherms can be used to assess the adsorption behaviour of the inhibitors. Langmuir adsorption isotherm is the best description of the adsorption behaviour of the inhibitor molecules on the mild steel surface [45], which obeys the following equation:

$$(C_{(inh)}/\theta) = C_{(inh)} + 1/K_{ads} \quad (5)$$

where (θ) is the surface coverage, (K_{ads}) is the adsorption–desorption equilibrium constant, and ($C_{(inh)}$) is the concentration of the inhibitor.
The surface coverage values (θ) were evaluated using corrosion rate values obtained from the weight loss method at ambient temperature. Coverage can be obtained from weight loss measurements by the following equation:

$$\theta = (W_{corr} - W'_{corr})/W_{corr} \quad (6)$$

where (W_{corr}) and (W'_{corr}) are the corrosion rates of steel with and without the inhibitors, respectively.
The corresponding plots are shown in Fig. 6, where the linear correlation (R^2) value for Langmuir isotherm was also nearly ***1*** for **D** and **D10**. From this observation, we concluded that Langmuir isotherm shows the best correlation with the experimental data. This kind of isotherm involves the monolayer adsorption characteristic and there is no interaction between the adsorbed inhibitor molecules and the carbon steel surface.
The free energy of adsorption ($\Delta G°_{ads}$) was calculated by the following equation:

$$\Delta G°_{ads} = -RT.ln(55.55\,K_{ads}) \quad (7)$$

where **55.55** is the molar concentration of water, ***R*** (**8.314 J/mol.K**) is the universal gas constant, *T* is the temperature in Kelvin and ($\mathbf{K_{ads}}$) is the adsorption–desorption equilibrium constant. Table 5 lists the thermodynamic parameters for the adsorption process

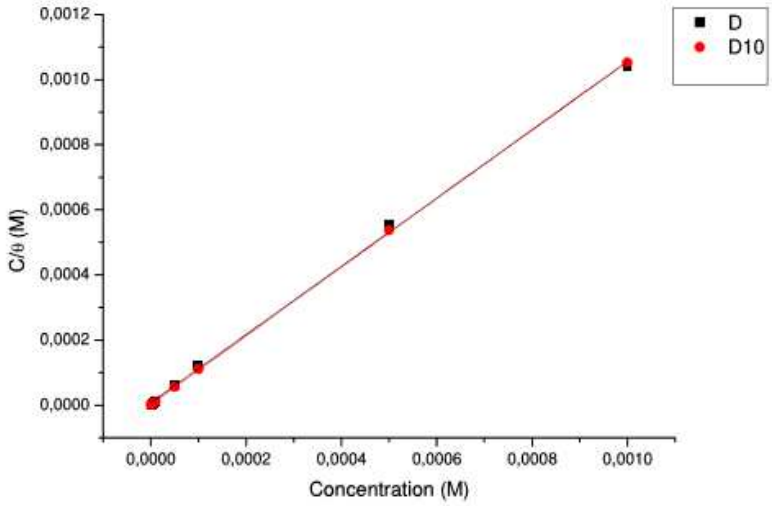

Figure 6. Langmuir adsorption of **D** and **D10** on the mild steel surface in 1 M HCl solution.

Table 5. Thermodynamic parameters for the adsorption of **D** and **D10** in 1 M HCl on mild steel surface at 25 °C.

Compounds	Linear correlation (R^2)	Slope	K_{ads}	$\Delta G°_{ads}$ (kJ mol^{-1})
D	0.9988	1.046	1.25×10^5	-40.347
D10	0.9998	1.053	3.41×10^5	-42.909

The negative value of $\Delta G°_{ads}$ indicates that the inhibitor is spontaneously adsorbed onto the mild steel surface. The values of $\Delta G°_{ads}$ calculated by Langmuir adsorption method for the inhibitors are **-40.3 kJmol^{-1}** for **D** and **-42,9 kJmol^{-1}** for **D10**. These values are at the interval of physisorption and chemisorption of the inhibitors on the steel surface [46]. Physisorption, where the electrostatic interaction assembled between the charged molecule and the charged metal, and chemisorption, where the Fe atoms on the metal surface formed bonds with an electron pair of nitrogen atoms presents in the organic inhibitor.

Quantum chemical calculations

The experimental studies confirm that **D** and **D10** are good inhibitors for the corrosion of mild steel in 1 M HCl. For explaining well the inhibiting efficiency of our inhibitors at the molecular level it is recommended to know the geometrical, energy and electronic properties of the inhibitors. These properties can be calculated using quantum chemical calculations (DFT) [47]. With this method we can calculate the energy gap (E_{gap}) between ionization potential (***IE***) and electron affinity (***EA***), dipole moment (μ), electronegativity (χ), global hardness (η), softness (σ) and fraction of electrons transferred (ΔN) which are presented in the Table 1.

According to the values of ***HOMO*** and ***LUMO*** energies of the two inhibitors, we note that these latter's are good donors and acceptors of electrons to the unoccupied 'd' orbital of the ion metal [28,31]. The high value of inhibitors dipole moment **μ(D)=3.6 Debye** and **μ(D10)=3.3 Debye** indicates the strong dipole–dipole interactions of the inhibitors and the metallic surface [48].The values of **ΔN** represent the number of electronic charges that will be exchanged between the surface and the adsorbed species. It is observed in this study that, the two values ΔN(**D**) and ΔN(**D10**) are almost equal, which confirms the good efficiency of our inhibitors [49].

Table 6. Molecular properties of **D** and **D10** from the optimized structure using '*DFT* ' at the *B3LYP/ 6-31G.*

Compounds		**D**	**D10**
μ	***Debye***	3.6051	3.3029
E_{HOMO}	***eV***	-5.1615	-5.1256
E_{LUMO}	***eV***	-0.072	-0.0205
EI	***eV***	5.1615	5.1256
EA	***eV***	0.072	0.0205
E_{gap}	***eV***	5.2335	5.1461
χ	***eV***	2.617	2.573
H	***eV***	2.54	2.57
σ	eV^{-1}	0.393	0.389
ΔN		0.8567	0.8613

The values of $EI(D)>EI(D10)$, $E_{gap}(D)>E_{gap}(D10)$ also $\mu(D)>\mu(D10)$ confirm that the efficiency of **D** is higher than the efficiency of **D10 [**50].
From the Table 6 we notice that there is a decrease in the ***EA*** and the dipole moment that justifies the difference of efficacy between **D** and **D10** which leads us to conclude that the integration of the methyl group in the position 3 slightly decreased the inhibiting efficiency with the conservation of the anticorrosive activity.
Table 6 presents the global reactivity indices calculated theoretically to **D** and **D10** molecules and the Fig. 7 presents the distributions of **HOMO-LUMO** frontier molecule orbital density of the same molecules.

Inhibition mechanism

Electrochemical and weight loss studies confirm that the compounds D and D10 inhibited the corrosion of mild steel in 1 M HCl through their adsorption at the metal/solution interface. The inhibitors are absorbed on the mild steel/hydrochloric acid solution interface by the following means [51,52]:

1. Electrostatic interaction of protonated inhibitor with already adsorbed chloride ions,
2. Donor–acceptor interactions between the π-electrons of aromatic ring and vacant d orbital of surface iron atoms,
3. Interaction between unshared electron pairs of heteroatoms of the inhibitor and vacant d orbital of iron surface atoms.

The calculated $\Delta G°_{ads}$ value of D and D10 ($|\Delta G°_{ads}| \geq 40$ kJ mol^{-1}) indicates that the adsorption of our inhibitors on the mild steel surface follows both physisorption (ionic) and chemisorption (molecular) mechanisms.

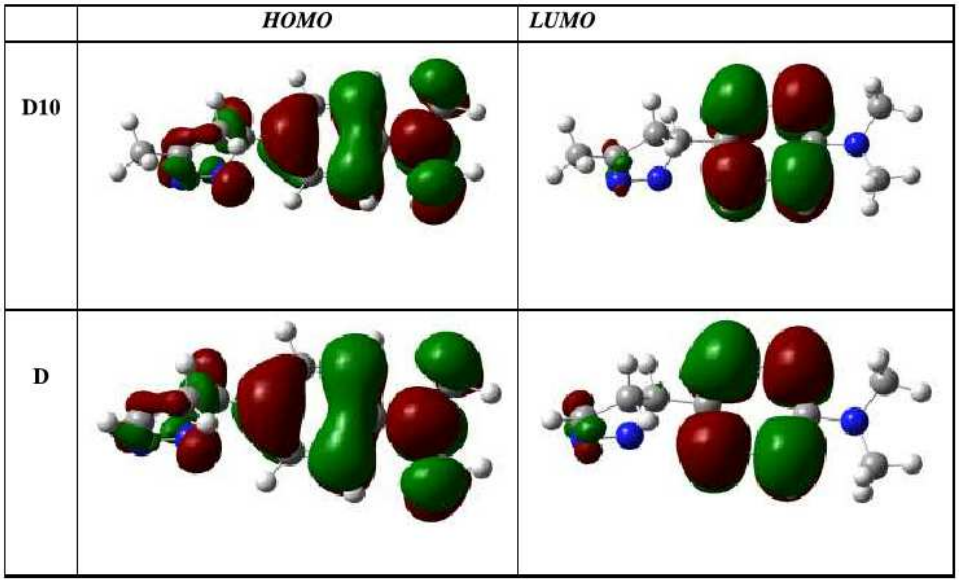

Figure 7. Distribution of the highest occupied molecular orbital ***HOMO*** and the lowest unoccupied molecular orbital ***LUMO*** in **D** and **D10** molecules.

Conclusions

In this work, we have realized the synthesis of two pyrazoles **D** and **D10** with good yield. IR and MNR (^{1}H and ^{13}C) spectra confirmed the chemical structures. The working studies of weight loss, electrochemical polarization and impedance spectroscopy show that ***D*** and ***D10*** were good mixed inhibitors (cathodic and anodic inhibitor) for corrosion of mild steel in 1 M HCl medium. Thermodynamic study and the theoretical calculations show that the adsorption mechanism of **D** and **D10** inhibitors on steel surface in 1 M HCl solution is due to physisorption and chemisorption. The integration of electronic effect inductive on or group as a methyl in the position three slightly decreased the inhibiting efficiency with the conservation of the anticorrosive activity. The computational chemistry results revealed that the compound **D** is more effective than **D10** and that they are both good corrosion inhibitors of steel in acid medium.

Acknowledgments

The authors are indebted to General Directorate for Scientific Research and Technological Development (Ministry of Higher Education and Scientific Research Algeria) and the laboratory of Chemistry and Environment (LCAE-URAC18), Faculty of Sciences, Oujda, Morocco, for financial support of this work.

References

1. Insuasty B, Tigreros A, Orozco F, et al. Bioorg Med Chem. 2010;18:4965.
2. El-Deeb M, Lee SH. Bioorg Med Chem. 2010;18:3961.
3. Holla BS, Akberali PM, Shivananda MK. IL Farmaco. 2000;*55*:256.
4. Manna F, Chementi F, Fioravanti R, et al. Bioorg Med Chem Lett. 2005;15:4632.
5. Ahn JH, Kim HM, Jung SH, et al. Bioorg Med Chem Lett. 2004;14:4461.
6. Ragavan RV, Vijayakumar V, Kumari NS. Eur J Med Chem. 2010;45:1173.
7. Jung JC, Watkins EB, Avery MA. Heterocycles. 2005;65:77.
8. Melnyk P, Leroux V, Sergheraert C, et al. Bioorg Med Chem Lett. 2006;16:31.
9. Sridhar K, Pandeya SN, Stables JP, et al. Eur J Pharm Sci. 2002;16:129.
10. Patole J, Sandbhor U, Padhye S, et al. Bioorg Med Chem Lett. 2003;13:51.
11. Rashad AE, Hegab MI, Abdel-Megeid RE, et al. Bioorg Med Chem. 2008;16:7102.
12. Siddiqui NJ, Idrees M, Khati NT, et al. S Afr J Chem. 2013;66:248.
13. Boudalia M, Bellaouchou A, Guenbour A, et al. Mor J Chem. 2014;2:97.
14. Benabdellah M, Yahyi A, Dafali A, et al. Arab J Chem. 2011;4:243.
15. Elayyachy M, Hammouti B, El Idrissi A, et al. Port Electrochim Acta. 2011;29: 57.
16. Zarrouk A, Warad I, Hammouti B, et al. Int J Electrochem Sci. 2010;5:1516.
17. El Ouali I, Hammouti B, Aouniti A, et al. J Mater Environ Sci. 2010;1:1.
18. Khaled KF, Abdelshafi NS, El-Maghraby A, et al. J Mater Environ Sci. 2011;2:166.
19. Aouniti A, Elmsellem H, Tighadouini S, et al. J Taibah Univ Sci. 2016;10:774.
20. Adejoro IA, Ojo FK, Obafemi SK. J Taibah Univ Sci. 2015;9:196.
21. Ben Hmamou D, Salghi R, Zarrouk A, et al. Ind Eng Chem Res. 2013;52:14315.
22. Zarrok H, Saddik R, Oudda H, et al. Der Pharm Chem. 2011;4:272.
23. Ghazoui, Saddik R, Benchat N, et al. Der Pharm Chem. 2012;4:352.
24. Al Hamzi AH, Zarrok H, Zarrouk A, et al. Int J Electrochem Sci. 2013;8:2586.
25. Goulart CM, Esteves-Souza A, Martinez-Huitle CA, et al. Corros Sci. 2013;67:281.
26. Redouane C, Bouhaous M, Naser A, et al. Asian J Materials Chem. 2016;1:33.
27. Avci G. Mater Chem Phys. 2008;112:234.
28. Meresht ES, Farahani TS, Neshati J. Corros Sci. 2012;54:36.
29. Chadli R, Elazouzi M, Khelladi I, et al. Port Electrochim Acta. 2017;35:65.
30. Corradi, Leonelli C, Rizzuti A, et al. Molecules. 2007;12:1482.
31. Mohareb RM, El-Sayed MNE, Abdelaziz MA. Molecules. 2012;17:18449.
32. Chadli R, ELhorri A, Elmsellem H, et al. Prot Metals Phys Chem Surf. 2017;53:928.
33. Frisch MJ, Trucks GW, Schlegel HB, et al. Gaussian, Inc., Wallingford, CT. 2010.

34. Becke AD. J Chem Phys. 1992;96:2155.
35. Becke AD. J. Chem. Phys. 1993;98:5648.
36. Lee C, Yang W, Parr RG. Phys. Rev. B. 1988;37:785.
37. Parr RG, Wang W. Density Theory for Atoms and Molecules. Oxford: Oxford University Press; 1989.
38. Parr RG, Szentpaly LV, Liu S. J Am Chem Soc. 1999;122:1922.
39. Yang W, Parr RG. Proc Nat Acad Sci. 1985;82:6723.
40. Uhrea J, Aramaki K. J Electrochem Soc. 1991;138:3245.
41. Mahgoub FM, Abdel-Nabey BA. Mater Chem Phys. 2010;120:104.
42. Salah M. Tawfik. J Mol Liq. 2015;207:185.
43. Atta AM, El-Azabawy OE, Ismail HS, et al. Corros Sci. 2011;53:1680.
44. Abdeli M, Ahmadi NP, Khosroshahi RA. J Solid State Electrochem. 2010;14:1317.
45. Morad MS. J Appl Electrochem. 2008;38:1509.
46. Zhao P, Zhong Ch, Hunag L, et al. Corros Sci. 2008;50:2166.
47. Amin MA, Khaled KF, Fadl-Allah SA. Corros Sci. 2010;52:140.
48. Ahamad I, Khan S, Ansari KR, et al. J Chem Pharm Res. 2011;3:703.
49. Migahed MA, Al-Sabagh AM, Khamis EA, et al. J Mol Liq. 2015;212:360.
50. Yadav M, Gope L, Kumari N, et al. J Mol Liq. 2016;216:78.
51. Quraishi MA, Jamal D. Mater Chem Phys. 2001;68:283.
52. Zarrouk A, Hammouti B, Lakhlifi T, et al. Corros Sci. 2015;90:572.